

An Explanation for Symmetry-Induced Isotopic Fractionation in Ozone

Gregory I. Gellene

Application of a theory of nuclear symmetry-based reaction restrictions to the $O_2 + O \rightarrow O_3$ reaction provides a potential explanation for the symmetry-induced isotopic enrichment observed for laboratory and atmospherically produced O_3 . Within this theory, the rate of formation of O_3 from collisions of O and isotopically homonuclear O_2 depends on whether the O_2 molecule is in an *f* (allowed) or an *e* (restricted) parity label state. The restriction can be relaxed by various potential energy surface coupling terms, and the assumption that approximately 78 percent of the restricted $O_2(e)$ levels produce O_3 with the same efficiency as the allowed $O_2(f)$ levels can account for laboratory-observed isotopic fractionation. In particular, the theory explains the special enhanced formation of the completely asymmetric isotopomer $^{16}O^{17}O^{18}O$.

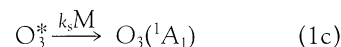
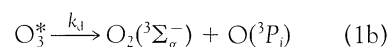
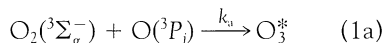
Symmetry-induced kinetic isotope effects (SIKIEs) are qualitatively and quantitatively different from the mass-dependent kinetic isotope effects normally considered in reaction dynamics; SIKIEs cause rate changes of a chemical process involving identical nuclei when the nuclear symmetry of the system is reduced by isotopic substitution. Because SIKIEs have their origin in symmetry rather than in mass considerations, large effects can, in principle, occur for all the elements in the periodic table.

One of the first chemical reactions for which a SIKIE was identified was the association reaction of O_2 and O to produce O_3 . The initial observation (1) was that stratospheric O_3 was enriched in ^{18}O up to 40% above its natural abundance level. After laboratory experiments (2) that showed that the enrichment occurs independently of isotopic mass (that is, $^{49}O_3$ and $^{50}O_3$ were nearly equally enriched), stratospheric measurements of $^{49}O_3$ (3) demonstrated that the enrichment occurring in the atmosphere was also independent of mass. The laboratory studies demonstrated that the extent of enrichment is affected by temperature, pressure, and the method of O atom production (4–8); however, to date, laboratory experiments have not produced the large enrichments observed in the stratosphere. Conversely, enrichment levels recently observed for tropospheric O_3 (9) are lower than the stratospheric values and are in agreement with the predictions from laboratory studies. Presently, despite more than 10 years of study, neither the fundamental role of symmetry nor the details of the isotopic fractionation mechanism in this important atmospheric reaction are understood.

In the last few years, SIKIEs have been investigated in several gas-phase ion stud-

ies (10). After the observation of an extraordinarily large SIKIE (~100) in the formation of O_4^+ by the trimolecular association of O_2^+ and O_2 (11), a general theory (12) of the phenomena was developed. Central to this theory is a symmetry correlation scheme that connects symmetry-distinct rovibronic states of the reactants with distinct electronic symmetries of the system in the interaction region, independent of the detailed geometry of the collision complex. When the system contains identical nuclei, the allowed reactant wave functions are restricted by the Pauli principle depending on the particular internal energy states involved. Thus, when the system contains asymptotic Born-Oppenheimer electronic state degeneracies, the propensity that the reactants will have for interacting on a particular Born-Oppenheimer potential energy surface (PES) can vary with the symmetry of the internal energy state of the reactants. However, reaction restrictions identified by this correlation scheme are based solely on the asymptotic states of the reactants. Because various PES coupling terms can mix these states, the extent to which the macroscopic kinetics will be modified by a predicted restriction depends on the "goodness" of an asymptotic description of the reactants at intermediate separations where the dynamics can be viewed as occurring on a particular PES. Application of this theory has led to the identification and interpretation of SIKIEs in the formation of He_2^+ , $(CO_2)_2^+$, and $Ar \cdot CO_2^+$ cluster ions (13–15).

The success of the SIKIE analysis of the ion-molecule clustering reactions provides strong support for the present theory of SIKIEs. This theory can be applied to the first step of the Chapman mechanism (16) for O_3 formation



where O_3^* is a collision complex, and k_d , k_d , and k_s are the phenomenological association, dissociation, and stabilization rate constants, respectively; O_2 and O_3 are in their ground electronic states, and the O atom can be in either its ground (3P_2) or first two excited (3P_1 , 3P_0) spin-orbit states. Because reaction 1a has a 27-fold Born-Oppenheimer degeneracy, the essential questions are whether nuclear symmetry can influence the PES on which the $O_2(^3\Sigma_g^-)/O(^3P)$ collisions occur and, if so, how isotopic substitution modifies the effect. By analogy with the study of SIKIEs in He_2^+ , O_4^+ , $(CO_2)_2^+$, and $Ar \cdot CO_2^+$ (11–15), I will address these questions in terms of an analysis of the nuclear-rotational-vibrational-electronic-translational wave function (Ψ_{nrvt}) for the infinitely separated $O_2(^3\Sigma_g^-) + O(^3P)$ supermolecule (denoted O_2/O) and the electronic wave functions (ϕ_e) of the O_3^* collision complex.

Using the coordinate system of (12) and noting that the $1s^2 2s^2 2p^4$ electron configuration of $O(^3P)$ is symmetric under coordinate inversion, I have written a zero-order wave function suitable for a symmetry analysis of O_2/O as the product of a diatomic wave function and a relative translational wave function. The latter is composed of a spherical Bessel function ($|J_L\rangle$) for the component of the translational wave function along the center of mass of O_2 and O, and a spherical harmonic ($|LM_L\rangle$) for the rotational component (17). The O_2 wave function can be written as a product of normalized Slater determinants of molecular orbitals ($|\dots\rangle$), harmonic oscillator vibrational wave functions ($|\nu\rangle$), and rotational wave functions. Taking into account spin-rotation interaction in the $^3\Sigma_g^-$ ground electronic state, Hund's case a functions ($|\Lambda/S\Sigma\rangle$ with $\Lambda = 0$, $S = 1$) and case b functions ($|I_a(A)I_b(B); I\rangle$) were used for the rotational and nuclear angular momentum wave functions of O_2 , respectively (18). The appropriate atomic nuclear spins ($I_{a,b}$) are 0

Table 1. Transformation properties of Ψ^\pm and Ψ^0 under the operations of $D_{\infty h}(M)$ (20).

Symmetry operation	Ψ^\pm	Ψ^0
E	Ψ^\pm	Ψ^0
(12)	$\mp(-1)^{J-S+I-2I_a}\Psi^\pm$	$-(-1)^{J-S+I-2I_a}\Psi^0$
E^*	$\mp(-1)^{J-S+L}\Psi^\pm$	$-(-1)^{J-S+L}\Psi^0$
(12)*	$(-1)^{I-2I_a+L}\Psi^\pm$	$(-1)^{I-2I_a+L}\Psi^0$

Department of Chemistry and Biochemistry, Texas Tech University, Lubbock, TX 79409, USA.

for ^{16}O and ^{18}O and $5/2$ for ^{17}O . Noting that the unpaired electrons in O_2 are in π_{g+} and π_{g-} molecular orbitals (12), I have written zero-order wave functions for O_2/O explicitly as

$$\Psi^0 = \frac{1}{\sqrt{2}} \{ |\pi_{g+}\bar{\pi}_{g-}| + |\bar{\pi}_{g+}\pi_{g-}| \} \times |J\Omega M_J\rangle |S\Sigma\rangle |v\rangle |I_n(A)I_n(B); I\rangle |LM_L\rangle |f_L\rangle \quad (2a)$$

$$\Psi^\pm = \frac{1}{\sqrt{2}} \{ |\pi_{g+}\pi_{g-}| |J\Omega M_J\rangle |S\Sigma\rangle \pm |\bar{\pi}_{g+}\bar{\pi}_{g-}| |J - \Omega M_J\rangle |S - \Sigma\rangle \} \times |v\rangle |I_n(A)I_n(B); I\rangle |LM_L\rangle |f_L\rangle \quad (2b)$$

where Ψ^0 is an $\Omega = 0$ level and Ψ^\pm are linear combinations of $\Omega = \pm 1$ ($\Omega = \Lambda + \Sigma$), and the absence or presence of a bar over the orbitals in the Slater determinants denotes an α or β spin-orbital, respectively. The symmetry properties of Eq. 2, a and b, are analyzed by permutation inversion (PI) group theory (19) and the molecular symmetry group of chemically feasible permutations is denoted $D_{\infty h}(M)$ (20). Using tables VII and VIII of (12), I found that Ψ^0 and Ψ^\pm are either unchanged or transformed into minus themselves under the operations of $D_{\infty h}(M)$ depending on the evenness or oddness of four angular momentum quantum numbers, $(J - S)$, I , $2I_n$, and L (Table 1). Because ^{16}O and ^{18}O are bosons and ^{17}O is a fermion, Ψ_{nrvert} must transform in $D_{\infty h}(M)$ as Σ_g^+ or Σ_u^- for $^{16}\text{O}^{16}\text{O}$ and $^{18}\text{O}^{18}\text{O}$ and as Σ_u^+ or Σ_g^- for $^{17}\text{O}^{17}\text{O}$. The Pauli-allowed asymptotic wave functions for collisions of isotopically

homonuclear O_2 with O are listed in Tables 2 and 3. If we follow the correlation scheme of (12), $\Psi_{\text{nrvert}} \rightarrow \phi_c$ is given by

$$\Psi^0 \rightarrow \phi_c^0 = \frac{1}{\sqrt{2}} (|\pi_{g+}\bar{\pi}_{g-}| + |\bar{\pi}_{g+}\pi_{g-}|) \quad (3a)$$

$$\Psi^\pm \rightarrow \phi_c^\pm = \frac{1}{\sqrt{2}} (|\pi_{g+}\pi_{g-}| \pm |\bar{\pi}_{g+}\bar{\pi}_{g-}|) \quad (3b)$$

Because the three O atoms can become equivalent in O_3^* , determining which ϕ_c (and thus which Ψ_{nrvert}) correlates with the ground electronic state of O_3 (A_1 in C_{2v} point-group symmetry) requires first determining the induced representation of ϕ_c in PI group $D_{3h}(M)$ (19) [$D_{\infty h}(M) \uparrow D_{3h}(M)$], and then determining the correlation of $D_{3h}(M)$ representations in the C_{2v} point group [$D_{3h}(M) \downarrow C_{2v}$]. In the last two columns of Tables 2 and 3, it can be seen that only $(J - S) = \text{even}$ states of $^{18}\text{O}^{18}\text{O}$ and $^{16}\text{O}^{16}\text{O}$ and $I = \text{even}$ and $(J - S) = \text{even}$ or $I = \text{odd}$ and $(J - S) = \text{odd}$ states of $^{17}\text{O}^{17}\text{O}$ correlate with the ground electronic state of O_3 . Because these states are the f parity label states, the correlation schemes in Tables 2 and 3 predict a symmetry restriction based on the eff parity label state of isotopically homonuclear O_2 . This finding is analogous to eff parity label state restrictions identified for O_4^+ , $(\text{CO}_2)_2^+$, and $\text{Ar} \cdot \text{CO}_2^+$ (11, 14, 15). No symmetry restrictions are predicted for collisions of isotopically heteronuclear O_2 and O because all levels correlate with the ground state of O_3 in this case.

The equilibrium statistical eff ratio is 2:1 for all isotopically homonuclear O_2 molecules (21). Thus, under conditions of $\bar{\text{O}}_2$ eff equi-

librium, the upper limit to isotopic enrichment of $^{49}\text{O}_3$ and $^{50}\text{O}_3$ resulting from this symmetry restriction is a factor of 2, which is more than sufficient to account for all laboratory and atmospheric observations. However, as discussed above, the symmetry restriction is by no means rigorous. The restriction is relaxed by mixing of the asymptotic O_2 ($J - S) = \text{even}$ levels with $(J - S) = \text{odd}$ levels at an intermediate O_2/O separation (Tables 2 and 3). In terms of the asymptotic wave function quantum numbers, this mixing can be accomplished by the angular momentum coupling term $\mathbf{J} \cdot (\mathbf{L} + \mathbf{j})$, where \mathbf{J} and \mathbf{j} are the total angular momentum (exclusive of nuclear spin) of O_2 and O, respectively, and \mathbf{L} is the orbital angular momentum of the O_2/O collision. This coupling provides a possible explanation for the observed temperature and pressure effects on laboratory isotopic enrichment (4-8), because the dynamical effects of the coupling may depend on the magnitude of \mathbf{J} and \mathbf{j} and on the relative velocity of O_2 and O. Further, a \mathbf{j} dependence for the coupling provides a possible mechanism for understanding the observed dependence on the method of O atom formation (4-8), which could produce varying distributions of 3P_2 , 3P_1 , and 3P_0 states.

Unfortunately, quantitative prediction of the strength of the symmetry restriction is difficult. Nevertheless, progress can be made by introducing an adjustable parameter (β) to account for the fraction of homonuclear $\text{O}_2(e)$ that overcomes the restriction. It is convenient to define a restriction factor (RF) that is equal to $(1 + 2\beta)/3$, $(7 + 2\beta)/9$, or 1 for the formation of O_3 containing one, two, or three different isotopes, respectively. Normalized to $^{48}\text{O}_3$, the

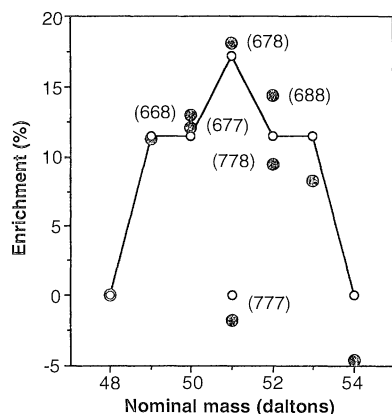


Fig. 1. Comparison of the experimental O_3 isotopic enrichment of Mauersberger *et al.* (8) (closed circles) and the present theoretical treatment with $\beta = 0.78$ (open circles). Numbers in parentheses indicate the O_3 isotopic composition (but not the structure) with "6," "7," and "8" signifying ^{16}O , ^{17}O , and ^{18}O , respectively.

Table 2. Correlation of Pauli-allowed wave functions for $^{32,36}\text{O}_2/\text{O} \rightarrow \text{O}_3^*$.

$J - S$	L	Ψ_{nrvert}	ϕ_e	$\Gamma(\phi_e)^\ddagger$	$\Gamma(\phi_e) \uparrow D_{3h}(M)$	$D_{3h}(M) \downarrow C_{2v}$
Even	Even	Ψ^-	ϕ_e^-	Σ_g^+	$A_1' \oplus E'$	$2A_1 \oplus B_2$
Even	Odd					
Odd	Even	Ψ^0	ϕ_e^0	Σ_g^-	$A_2'' \oplus E''$	$2A_2 \oplus B_1$
Odd	Odd					

‡ Irreducible representation of ϕ_e in $D_{3h}(M)$ symmetry.

Table 3. Correlation of Pauli-allowed wave functions for $^{34}\text{O}_2/\text{O} \rightarrow \text{O}_3^*$.

I	$J - S$	L	Ψ_{nrvert}	ϕ_e	$\Gamma(\phi_e)^\ddagger$	$\Gamma(\phi_e) \uparrow D_{3h}(M)$	$D_{3h}(M) \downarrow C_{2v}$
Even	Even	Even	Ψ^-	ϕ_e^-	Σ_g^+	$A_1' \oplus E'$	$2A_1 \oplus B_2$
Even	Even	Odd					
Odd	Odd	Even					
Odd	Odd	Odd	Ψ^0	ϕ_e^0	Σ_g^-	$A_2'' \oplus E''$	$2A_2 \oplus B_1$
Even	Odd	Even					
Even	Odd	Odd					

‡ Irreducible representation of ϕ_e in $D_{3h}(M)$ symmetry.

theoretical percent enrichment for O_3 of isotopic composition (ijk) is given by $[RF^{(ijk)O_3}/RF^{(48O_3)} - 1] \times 100\%$. A particularly significant comparison can be made to the experimental results of Mauersberger *et al.* (8), who measured isotope enrichment for all isotopomers of O_3 using oxygen enriched in ^{17}O and ^{18}O (22). The best agreement was achieved for $\beta = 0.78$ (Fig. 1). Using this value for β , RFs of 0.85 and 0.95 were determined for $^{48}O_3$ and $^{49,50}O_3$, respectively, which compares well with the available experimental results. Uniform agreement with the various laboratory and atmospheric measurements is not expected for at least four reasons. First, the observed isotopic enrichments, and therefore β in this model, vary with experimental conditions. Second, no account was taken of mass-dependent kinetic isotope effects. The importance of this effect is shown by the experimentally observed depletion of $^{17}O^{17}O^{17}O$ and $^{18}O^{18}O^{18}O$ relative to $^{16}O^{16}O^{16}O$ (Fig. 1) in accord with theoretical predictions (23). Third, the possibility of isotopic exchange when M in reaction 3c is O_2 was not considered. Fourth, possible SIKIEs in reactions 3b or 3c were not considered. This last point may be significant because there is some experimental evidence (13, 14) that a decrease in symmetry may enhance the energy transfer stabilization step of the formation mechanism. This effect may be relevant to the enhanced production of $^{16}O^{16}O^{18}O$ relative to $^{16}O^{18}O^{16}O$ observed in some laboratory (24) and atmospheric (25–28) measurements.

Earlier theoretical treatments have attempted to rationalize SIKIEs in O_3 formation in terms of incomplete energy randomization in O_3^* or in terms of excited-state curve crossings (29, 30) but could not account for the special enrichment of the completely asymmetric isotopomer. This enrichment can be rationalized within the conceptual framework presented in this report. The present explanation differs qualitatively from earlier approaches by focusing on the symmetry properties of the infinitely separated $O_2 + O$ reactants and how they correlate with those of O_3^* instead of considering the O_3^* complex only. The interpretation that $^{32}O_2(f)$ produces $^{48}O_3$ more efficiently than $^{32}O_2(e)$ implies by microscopic reversibility that thermal dissociation of $^{48}O_3$ will preferentially produce $^{32}O_2(f)$ over $^{32}O_2(e)$. The experimental investigation of this prediction would provide a stringent test of the theory.

REFERENCES AND NOTES

1. K. Mauersberger, *Geophys. Res. Lett.* **8**, 935 (1981).
2. M. H. Thiemens and J. E. Heidenreich III, *Science* **219**, 1073 (1983).
3. B. Schueler, J. Morton, K. Mauersberger, *Geophys. Res. Lett.* **17**, 1295 (1990).
4. J. Yang and S. Epstein, *Geochim. Cosmochim. Acta* **51**, 2019 (1987).
5. M. H. Thiemens and T. Jackson, *Geophys. Res. Lett.* **15**, 639 (1988).
6. J. Morton, B. Schueler, K. Mauersberger, *Chem. Phys. Lett.* **154**, 143 (1989).
7. M. H. Thiemens and T. Jackson, *Geophys. Res. Lett.* **17**, 717 (1990).
8. K. Mauersberger, J. Morton, B. Schueler, J. Stehr, S. M. Anderson, *ibid.* **20**, 1031 (1993).
9. D. Krankowsky, F. Bartelck, G. G. Klees, K. Mauersberger, K. Schellenbach, *ibid.* **22**, 1713 (1995).
10. G. I. Gellene, in *Advances in Gas Phase Ion Chemistry*, vol. 2, N. G. Adams and L. M. Babcock, Eds. (JAI Press, Greenwich, CT, 1996), pp. 161–191.
11. K. S. Griffith and G. I. Gellene, *J. Chem. Phys.* **96**, 4403 (1992).
12. G. I. Gellene, *ibid.*, p. 4387.
13. ———, *J. Phys. Chem.* **97**, 34 (1993).
14. R. K. Yoo and G. I. Gellene, *J. Chem. Phys.* **102**, 3227 (1995).
15. ———, *ibid.* **105**, 177 (1996).
16. S. Chapman, *Philos. Mag.* **10**, 345 (1930).
17. L is the quantum number of the relative orbital angular momentum (L) of O_2 and O and M_L is the projection of L on a space-fixed z axis.
18. Hund's case (a) rotational angular momentum wave functions are labeled by projection of the total electronic orbital angular momentum on the molecule-fixed z axis (A), the total angular momentum exclusive of nuclear spin (J), the total electron spin angular momentum (S), and the projection of the total electron spin angular momentum on the molecule-fixed z axis (Σ). Hund's case (b) nuclear angular momentum wave functions are labeled by the atomic nuclear spin of atoms A and B [$I_A(A)$ and $I_B(B)$, respectively] and the total molecular nuclear spin (I).
19. P. R. Bunker, *Molecular Symmetry and Spectroscopy* (Academic Press, New York, 1979).
20. The operations of $D_{2h}(M)$ as applied to the O_2/O supermolecule are the identity, permutation of the atoms in O_2 , inversion of all coordinates, and permutation of the atoms in O_2 followed by inversion of all coordinates. They are denoted E , (12) , E^* , and $(12)^*$, respectively (Table 1).
21. The statistical ef ratio is determined most simply by considering Hund's case (b) rotational angular momentum wave functions where N , the total angular momentum exclusive of nuclear and electron spin, replaces Σ of Hund's case (a) rotational wave functions. In general, with $S = 1$, there are three values of J ($N - 1$, N , and $N + 1$) for each value of N . Two of these three J levels are e states, and the third is an f state.
22. In contrast to Morton *et al.* (6) and Mauersberger *et al.* (8), J. Yang and S. Epstein [*Geochim. Cosmochim. Acta* **51**, 2011 (1987)] reported no symmetry-dependent isotope effects using O_2 highly enriched in ^{17}O and ^{18}O . However, it may be significant that Yang and Epstein converted O_3 to O_2 before isotopic analysis, whereas Morton *et al.* and Mauersberger *et al.* isotopically analyzed O_3 directly.
23. J. A. Kaye, *J. Geophys. Res.* **91**, 7865 (1986).
24. S. M. Anderson, J. Morton, K. Mauersberger, *Chem. Phys. Lett.* **156**, 175 (1989).
25. C. P. Rinsland *et al.*, *J. Geophys. Res.* **90**, 10719 (1985).
26. A. Goldman *et al.*, *ibid.* **94**, 8467 (1989).
27. A. Meier and J. Notholt, *Geophys. Res. Lett.* **23**, 551 (1996).
28. F. W. Irion *et al.*, p. 2377.
29. D. R. Bates, *J. Chem. Phys.* **93**, 8739 (1990).
30. J. J. Valentini, *ibid.* **86**, 6757 (1987).
31. This research was supported by the National Science Foundation (CHE95-51008) and the Robert A. Welch Foundation. This material is based in part on work supported by the Texas Advanced Research Program under grant 003644-071.

19 July 1996; accepted 10 October 1996

Oceanic Carbon Dioxide Uptake in a Model of Century-Scale Global Warming

Jorge L. Sarmiento* and Corinne Le Quére

In a model of ocean-atmosphere interaction that excluded biological processes, the oceanic uptake of atmospheric carbon dioxide (CO_2) was substantially reduced in scenarios involving global warming relative to control scenarios. The primary reason for the reduced uptake was the weakening or collapse of the ocean thermohaline circulation. Such a large reduction in this ocean uptake would have a major impact on the future growth rate of atmospheric CO_2 . Model simulations that include a simple representation of biological processes show a potentially large offsetting effect resulting from the downward flux of biogenic carbon. However, the magnitude of the offset is difficult to quantify with present knowledge.

The most important anthropogenic greenhouse gas contributing to increased radiative trapping today and in the foreseeable future is CO_2 (1). International agreements to mitigate increased radiative trapping have begun to take the form of atmospheric CO_2 stabilization scenarios, such as those examined in a recent Intergovernmental Panel on Climate Change (IPCC) study (2–4). The major sinks for anthropogenic CO_2 emis-

sions are the ocean and the terrestrial biosphere. The oceanic sink in the IPCC stabilization scenarios was calculated based on the assumption that the ocean circulation and temperature will remain constant over the next few centuries. However, Manabe and Stouffer (5, 6) have shown that the global warming resulting from increased CO_2 concentrations may have a significant effect on ocean circulation and temperature. Here, we examine the effects of such changes on oceanic CO_2 uptake, using the coupled ocean-atmosphere global warming model of Manabe and Stouffer (5).

Program in Atmospheric and Oceanic Sciences, Princeton University, Princeton, NJ 08544, USA.

*To whom correspondence should be addressed.